Journal of the Ceramic Society of Japan 118 [9] 805-809 2010 Paper

Effect of CTAC concentration and Al precursor type on texture properties and microstructure of mesoporous alumina particles prepared by aerosol-assisted self-assembly

Joo Hyun KIM, Kyeong Youl JUNG† and Kyun Young PARK

Department of Chemical Engineering, Kongju National University, 275 Budae-dong, Cheonan, Chungnam 330–717, Republic of Korea

The effect of the CTAC/Al ratio and the Al precursor type on the texture properties of alumina prepared by the evaporation-induced self-assembly (EISA) of aerosols was studied using N_2 adsorption isotherms, small-angle X-ray scattering (SAXS), scanning electron microscopy (SEM), and transmission electron microscopy (TEM). For the CTAC/Al ratio range 0.05 < CTAC/Al < 0.5 the prepared alumina particles had worm-like pore structure with a BET surface area of 170–365 m^2/g and pore size of 2.7–3.4 nm. At CTAC/Al = 0.3, the largest surface area was achieved. The chloride precursor was most profitable to obtain the largest surface area (~365 m^2/g). However, the nitrate precursor was better for preparing non-hollow and mesoporous alumina, maintaining high surface area (~320 m^2/g) and pore regularity.

Key-words : Mesoporous, Al_2O_3, Aerosol method, CTAC, Self assembly

[Received April 7, 2010; Accepted July 15, 2010]

1. Introduction

In ceramic industry, alumina is a very attractive material with important applications in the ultrafiltration of salts, as a catalyst or as a heterogeneous catalyst support for automobiles or petroleum refinement, and as an absorbent for environmental cleanup.[1)–3)] In most industrial applications, the alumina is required to have a high surface area and pore volume, well-defined pores with a narrow size distribution, and proper particle size and morphology. Thus, many efforts have been devoted to prepare mesoporous alumina with regular pore structure.[4)–7)]

Mesoporous alumina oxides have been synthesized through the template approaches such as sol–gel processes,[8)] evaporation-induced self-assembly (EISA),[9)] and spray pyrolysis.[10)] Čejka described the state of the art of the synthesis and potential of mesoporous alumina.[11)] Evaporation-induced self assembly in an aerosol reactor was reported as a simple and effective method to prepare powders with a highly ordered hexagonal meso-phase.[12)–16)] In the conventional liquid-phase synthesis, the self-assembly occurs quickly, but a time scale of days or longer is required to ensure a high degree of order in mesopores. In comparison, the aerosol route can induce self assembly with a process time of only several seconds or less, especially using a relatively non-expensive precursor like metal salts. The aerosol-assisted EISA process compared to the traditional solution methods also has other several attractive points: the process is continuous and can be easily increased in scale, the particles produced generally have a spherical shape, and especially the uniform incorporation into mesoporous particles of every chemical species that can be dissolved or dispersed into a precursor solution.[14)] Most studies using EISA of aerosols, however, have focused on silica particles. Tsung et al. also prepared highly ordered metal oxides with highly crystalline frameworks via the aerosol route combined with the acetic acid mediated sol–gel system using alkoxide precursors and amphiphilic copolymer F127 ($EO_{106}PO_{70}EO_{106}$).[17)] The alkoxide precursor, however, is more expensive than Al salt precursors such as nitrate, chloride, and acetate. Recently, Grosso et al. used a spray drying method to prepare alumina mesoporous spheres using $AlCl_3 \cdot 6H_2O$ and $[E(B)]_{75}$-$[EO]_{86}$ block copolymer as the Al precursor and the templating agent, respectively.[18)] The texture properties of mesoporous alumina could be influenced by the Al precursor type. To the best of our knowledge, no study on the effect of Al salt precursor types on the texture properties of alumina prepared by the aerosol-assisted EISA process has been reported, especially using cetyltrimethylammonium chloride (CTAC) as a structure-directing agent. In this work, therefore, mesoporous alumina particles were prepared by the aerosol-assisted EISA process using both CTAC surfactant and various aluminum salts such as nitrate, chloride, and acetate. Then, the texture properties, the morphology, and the microstructure of alumina particles with varying CTAC content and different types of aluminum precursors were systematically studied by using N_2 isotherms, small-angle X-ray scattering measurements, and scanning or transmission electron microscopy. On the basis of the results, we demonstrated in detail the nature of the pore and particle formation in an aerosol reactor.

2. Experimental

2.1 Preparation of mesoporous alumina using the EISA of aerosols

Three types of aluminum salts, nitrate ($Al(NO_3)_2 \cdot 9H_2O$, Aldrich, 99.9%), chloride ($AlCl_3 \cdot 6H_2O$, Aldrich, 99%), and acetate ($Al(OH)(C_2H_3O_2)_2$, Aldrich), were used as the starting materials. Cetyltrimethylammonium chloride (CTAC, Aldrich, 25 wt %) was used as a structure-directing agent. The following is a typical procedure for the preparation of the precursor solution. The aluminum precursors were dissolved in 250 mL of purified

† Corresponding author: K. Y. Jung; E-mail: kyjung@kongju.ac.kr

water with urea (Aldrich, 98%), and the concentration was fixed at 0.6 M. Then, in a second beaker, the CTAC surfactant was dissolved in 250 mL of water at 30°C under vigorous stirring. Subsequently, the two solutions were mixed to obtain a homogeneous spray solution. The concentration of aluminum precursor in the final spray solutions (500 mL) was fixed at 0.2 M. The molar ratio of urea to the Al precursor was also fixed at 3 in all the spray solutions. The molar ratio of surfactant to the aluminum precursor, CTAC/Al, was varied from 0.05 to 0.5 in order to find the optimal concentration at which the highest surface area could be obtained.

The precursor solutions prepared above were atomized by an ultrasonic aerosol generator with 7 vibrators at 1.7 MHz. Subsequently, the droplets produced were carried by air (20 *l*/min) into a quartz reactor (i.d. = 55 mm, length = 1000 mm) equipped with two-zone electric heaters. The first half of the reactor was maintained at 150°C, and the other was kept at 500°C. At the end of the reactor, the alumina precursor powder was collected by a Teflon bag filter and calcined at 550°C for 4 h.

2.2 Characterization

For the calcined samples, nitrogen adsorption/desorption isotherms were measured at 77 K using a Microelectronics ASAP 2010 apparatus. All the samples were outgassed under vacuum at 250°C for 2 h prior to measurement. The specific surface areas were calculated according to the BET (Brunauer–Emmett–Teller) equation. The pore size distributions were calculated using the Barret–Joyner–Halenda (BJH) model. The pore volume was taken from the adsorbed amount at a relative pressure of 0.99. Small-angle X-ray diffraction (SAXS) patterns were recorded on Rigaku D/Max-2500 diffractometer. Scanning electron microscopy (SEM. JMS 6360) and transmission electron microscopy (TEM, Philips Tecnai F20) were used to investigate the morphology and the microstructure of prepared mesoporous alumina samples.

3. Results and discussion

3.1 Effect of CTAC/Al ratio on the texture properties

Figure 1 shows the N_2 adsorption–desorption isotherms and the pore size distributions of the alumina particles prepared from the nitrate precursor by changing the CTAC/Al ratios. All the samples prepared showed a typical type IV isotherm, indicating that the Al_2O_3 particles prepared were mesoporous materials. According to IUPAC classification of adsorption isotherms,[19] there are four types of hysteresis loops, designated as H1, H2, H3, and H4. At CTAC/Al = 0.05, 0.4, and 0.5, the alumina particles had a typical H2 hysteresis loop related to the capillary condensation associated with mesoporous channels. When the CTAC/Al ratio was 0.1–0.2, the particles showed type IV features with no hysteresis loop, typical of relatively monodispersed pores. As shown in Fig. 1(b), the pore size distributions showed a maximum peak at about 3.5 nm in all samples, indicating that the size of most CTAC micelles formed in droplets is nearly constant regardless of the CTAC/Al ratio.

The BET surface area, pore volume, and average pore size are summarized in **Table 1**. Compared with the sample prepared without the template (CTAC/Al = 0.0), a substantial increase in the BET surface area was observed at CTAC/Al ≥ 0.1, due to the mesopores formed by the removal of CTAC templates. There was no significant change in the average pore size, which was determined using the BJH method. The largest surface area, 320 m^2/g, was obtained at CTAC/Al = 0.3, although the largest

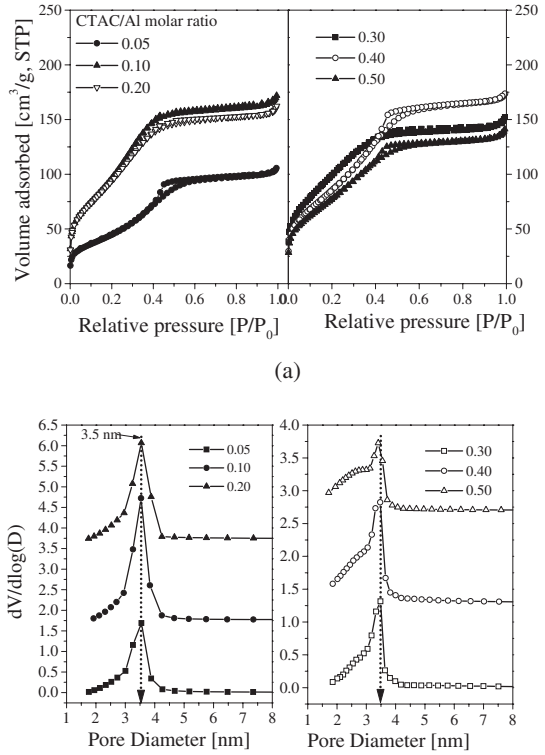

Fig. 1. (a) Nitrogen adsorption/desorption isotherms and (b) pore size distributions for mesoporous alumina powders produced by changing the CTAC/Al ratio.

Table 1. Summary of the texture properties for mesoporous alumina prepared using various CTAC/Al molar ratios

CTAC/AL	S_{BET} [m^2/g]	V_p [a)] [cm^3/g]	d_{BJH} [b)] [nm]	d_{100} [c)] [nm]
0.0	11	0.022	7.9	—
0.05	178	0.163	3.4	8.8
0.1	300	0.266	3.4	8.4
0.2	292	0.251	3.4	7.4
0.3	320	0.236	2.7	6.5
0.4	260	0.269	3.0	7.1
0.5	244	0.218	2.8	7.3

a) The pore volumes of the samples were determined at $P/P_0 = 0.995$.
b) The mean pore sizes of the samples were calculated by the BJH equation from the desorption isotherms.
c) d spacing between (100) plans, calculated from the SAXS peak.

pore volume was observed at CTAC/Al = 0.4. As shown in Fig. 1(a), the adsorption volume greatly increased with increasing CTAC/Al ratio from 0.05 to 0.1. In addition, the H2 type hysteresis loop observed at CTAC/Al = 0.05 disappeared at CTAC/Al = 0.1. Thus, most of the CTAC molecules added are assumed to be involved in the formation of mesopores in the alumina matrix. No large difference in the surface area was observed for CTAC/Al ratios of 0.1 to 0.3. When the CTAC/Al ratio was over 0.4, however, the surface area was reduced rather than increased. From the results, it was clear that the aerosol process is an effective method to obtain mesoporous alumina with a high surface area even at a low CTAC concentration. In addition, some of the CTAC molecules at high concentration did not contribute to making the mesopores, and instead, they lowered the surface area when the content was more than a certain quantity.

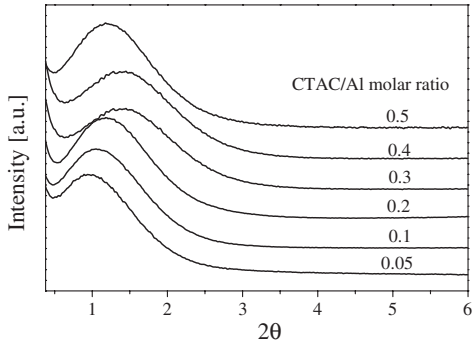

Fig. 2. Small-angle X-ray scattering (SAXS) curves for alumina powders prepared by changing the CTAC/Al ratio.

Figure 2 shows small-angle X-ray diffraction patterns of the mesoporous alumina prepared by the aerosol process with varying CTAC/Al ratio. All the samples showed a single peak around $2\theta = 0.5$–$3°$, related to the presence of well-organized regular mesopores. There were no further reflections indicating hexagonal or cubic symmetry. Thus, the alumina particles had disordered worm- or sponge-like mesostructures.[20),21)] One notable feature is the SAXS peak positions, which change with the quantity of surfactant. As the CTAC/Al ratio increased from 0.05 to 0.3, the position of the SAXS peak shifted toward the larger angle side: from $2\theta = 0.95°$ to $2\theta = 1.73°$. Conversely, the peak shifted again toward the smaller angle side at CTAC/Al ≥ 0.3. The peak positions in the SAXS patterns are related to the d-spacing value, representing a distance between the pores and related to the pore size and wall thickness. The d-spacing values of the mesoporous alumina were calculated by the XRD peak at the (100) reflection and are summarized in Table 1. Under the assumption that the size of micelles is fixed and all the CTAC surfactant added is involved in making pores, the surface area should increase with increasing CTAC/Al ratio, reducing the distance between pores. As a result, the SAXS peak should shift to a larger angle, reducing the d-spacing value with increasing CTAC/Al ratio. As shown in Table 1, the increase of the CTAC/Al ratio from 0.05 to 0.3 led to the increase in the surface area and the reduction in the d-spacing value from 8.8 to 5.5 nm, theoretically, in good agreement with the shift in the SAXS peak to a larger angle, as shown in Fig. 2. The d-spacing value increased again when the CTAC/Al ratio was larger than 0.3, reflecting the loss of the pore density (# of pores per unit particle volume) and in good agreement with the appearance of the shoulder peak in the pore size distribution shown in Fig. 1(b).

3.2 Effect of the Al precursor type on the texture properties

Figure 3 shows the nitrogen isotherms and the pore size distributions of the mesoporous alumina prepared by changing the Al precursor type. The Al precursor type strongly influenced the saturation volume as well as the shape of the isotherm, which indicates that the pore morphology changed. The acetate precursor gave the largest saturation pore volume, but the adsorbed volume was smallest for relative pressures $P/P_0 < 0.4$. The isotherm type IV was observed regardless of the precursor types, but the hysteresis loop was different. No hysteresis loop was observed for the nitrate precursor, whereas a typical H2 hysteresis loop appeared for the chloride and acetate precursors. In particular, two hysteresis loops appeared for the acetate precursor, indicating that pores with different sizes were formed.

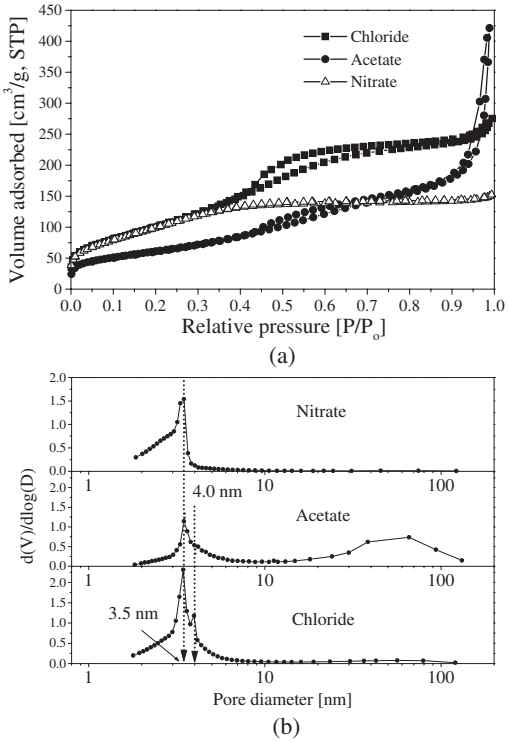

Fig. 3. Effect of Al precursor types on N_2 adsorption/desorption isotherms (a) and pore size distributions (b). In all precursor solutions, the CTAC/Al ratio was 0.3.

Table 2. Texture properties of alumina prepared by changing the Al precursor type

Precursor	S_{BET} [m^2/g]	V_p [cm^3/g]	d_{BJH} [nm]	d_{100} [nm]
Chloride	365	0.387	3.8	10.2
Acetate	222	0.628	10.2	—
Nitrate	320	0.236	2.7	6.5

Thus, as shown in Fig. 3(b), two peaks were observed for the acetate precursor: one is at 3.5 nm, and the other is at 60–70 nm. It was notable that the main peak of the pore size distribution remained at 3.5 nm regardless of the Al precursors. The texture properties of the alumina prepared by changing the Al precursor type were summarized in **Table 2**. The largest surface area, 365 m^2/g, was achieved when the chloride precursor was used.

Figure 4 shows the SAXS results of the mesoporous alumina prepared by changing the Al precursors. The alumina particles prepared using the nitrate and the chloride precursor had a clear peak due to the presence of well-organized regular mesopores. For the acetate precursor, however, no SAXS peak appeared, indicating that the alumina had mesopores with not only a low regularity in size but also a broad size distribution, as shown in Fig. 3(b). When considering the SAXS-peak position, the chloride precursor was found to have the SAXS peak at a smaller diffraction angle compared with the nitrate one. As a result, the alumina produced by the chloride precursor showed a larger d-spacing value than that produced by the nitrate precursor. When the CTAC concentration is fixed, the enlargement of the d-spacing value can be achieved for two reasons: one is the increase in pore size and the other is the reduction in the number of spherical micelles involved in making the pores. Referring to the fact that the mesopores are formed by the CTAC micelles, the

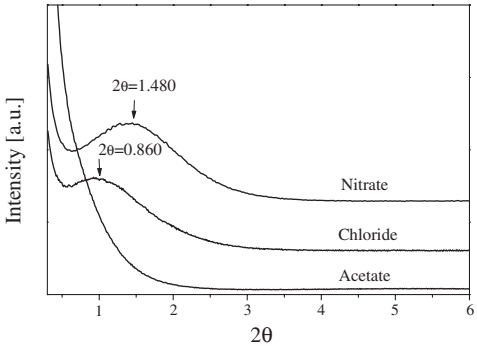

Fig. 4. Small-angle X-ray scattering (SAXS) curves of alumina powders prepared by changing the Al precursor type.

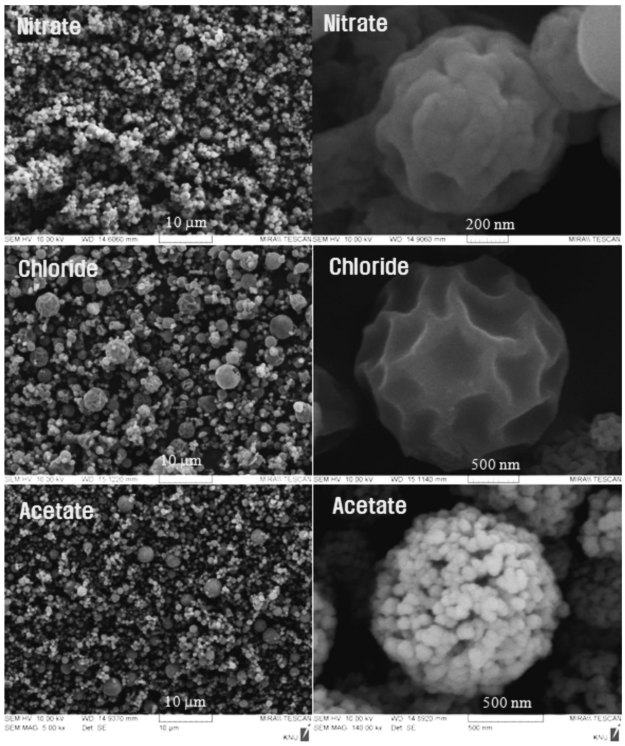

Fig. 5. Scanning electron micrographs for mesoporous alumina particles prepared by changing the Al precursor type at CTAC/Al = 0.3.

surface area is basically related to the number of micelles involved in making the mesopores. Then, it is acceptable that the chloride precursor compared with the nitrate had more spherical CTAC micelles involved in the pore generation because the surface area for the chloride precursor was larger than that for the nitrate.

3.3 SEM and TEM analysis

Figure 5 shows SEM photos for the alumina particles prepared using three different precursors. All particles had a spherical shape regardless of the type of precursor. The alumina prepared from the chloride precursor had a relatively bad morphology and many large particles differentiable with the naked eye, compared with those prepared from the other two precursors. In the aerosol pyrolysis process, the particle size mainly depends on the concentration of the aluminum precursor and the average size of the droplets. The droplet size is determined mainly by the frequency of the ultrasonic vibrators,

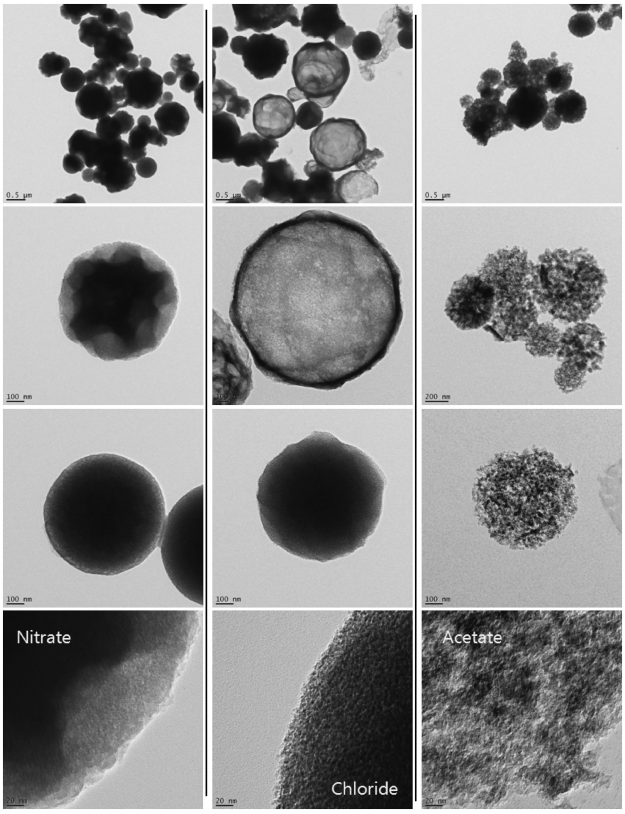

Fig. 6. Transmission electron micrographs for mesoporous alumina particles prepared by changing the Al precursor type at CTAC/Al = 0.3.

which, in this work, were fixed at 1.7 MHz. Thus, there is no significant change in the droplet size. The concentrations of the aluminum precursors were also fixed. Therefore, the particle size is assumed not to change due to the precursor type. Nevertheless, the observation even with the naked eye for the relative large particles shows that many hollow-structured particles were generated when using the chloride precursor and is in agreement with the TEM analysis below. On the base of magnified photographs displayed on the right side in Fig. 5, the surface morphology differed with precursor type. For the nitrate and chloride precursors, the small-sized particles had a completely round shape, whereas the relative large particles had a dimpled surface. For the acetate precursor, the prepared particles were the aggregation of many primary particles, each less than several tens of nanometers.

The effect of the precursor type on the morphology and the microstructure was clearly indentified in the TEM pictures in **Fig. 6**. The alumina particles prepared from the nitrate precursor had a filled morphology and some particles showed a dimpled shape. In the case of the chloride precursor, the relatively large particles had hollow structure with a porous shell, but the filled morphology was also observed in relatively small particles. When the acetate precursor was used, the prepared particles showed a different microstructure compared with other two precursors. As identified in the SEM photos, the TEM picture for the acetate precursor indicates that the prepared alumina particles exist as an aggregation consisting of nanoparticles and have many macropores observable with the naked eye, which is in good agreement with the pore size distribution in Fig. 3(b). It was also confirmed that no ordered-mesopore structure was formed in any of the precursors.

In the aerosol process, the precipitation characteristics of salts are critical to determine the particle morphology. The hollow morphology is produced when local precipitation occurs, whereas the filled morphology is obtained by volumetric precipitation during the drying step. The precipitation behavior is affected mainly by the solubility of aluminum precursors and the drying rate. In this work, the temperature of the aerosol reactor and the flow rate of the carrier gas were fixed, indicating that the drying rate could be considered as a constant for all the precursors. Thus, the solubility of each precursor is a critical factor to determine the particle morphology and whether during the drying step more micelles are formed from the CTAC molecules or not. The solubility of the Al precursors used is in the following order: nitrate (160 g/100 mL @ 100°C) > chloride (49 g/100 mL @ 100°C) > acetate (appreciable). Thus, the nitrate precursor rather than the chloride or the acetate ones has the advantage of avoiding local precipitation during the drying of droplets. Thus, as shown in Fig. 6, the filled morphology for the nitrate precursor was obtained. For the chloride precursor, most of particles also have a non-hollow structure, except for the relatively large particles, which were mainly produced from the large droplets. For the acetate precursor, the colloid particle-like opaque milk was initially formed in the precursor solution. Thus, the aggregates of nanoparticles were formed as shown in Fig. 5 and Fig. 6.

4. Conclusions

Mesoporous alumina particles with spherical shape were successfully prepared by the evaporation-induced self-assembly of aerosols using aqueous solutions of CTAC and aluminum salts such as nitrate, chloride, and acetate. It was confirmed that the CTAC/Al ratio significantly influenced the surface area and the pore volume of the alumina particles. According to the SAXS analysis, a clear peak was found at $2\theta = 1$–$2°$ due to the generation of the well-organized regular mesopores, but no further peak indicating the structural ordering of mesopores was observed. In the CTAC/Al ratio range from 0.05 to 0.3, the SAXS peak shifted to a larger angle with increasing CTAC content, which can be explained by the reduction in the distance between CTAC micelles with the increasing number density of CTAC micelles involved in the formation of pores. The particle morphology and the texture properties of alumina were strongly affected by the Al precursor type. The N_2 isotherms and SAXS results indicated that the chloride precursor is the most profitable to prepare mesoporous alumina with the largest BET surface area ($365\,m^2/g$) and pore volume ($0.387\,cm^3/g$). From the SEM and TEM analysis, the nitrate precursor is better than the others for obtaining a completely filled morphology with high surface area and well-organized regular pores.

Acknowledgment This research was supported by a grant from the Fundamental R&D Program for Core Technology of Materials funded by the Ministry of Knowledge Economy, Republic of Korea.

References

1) P. A. Zieliński, R. Schulz, S. Kaliaguine and A. Van Neste, *J. Mater. Res.*, 8, 2985–2992 (1993).
2) J. Schaep, C. Vandecasteele, B. Peeters, J. Luyten, C. Dotremont and D. Roels, *J. Membr. Sci.*, 163, 229–237 (1999).
3) Y. Kim, C. Kim, I. Choi, S. Rengaraj and J. Yi, *Environ. Sci. Technol.*, 38, 924–931 (2004).
4) K. Niesz, P. Yang and G. A. Somorjai, *Chem. Commun.*, 15, 1986–1987 (2005).
5) J. Aguado, J. M. Escola and M. C. Castro, *Microporous Mesoporous Mater.*, 128, 48–55 (2010).
6) B. Xu, J. Long, H. Tian, Y. Zhu and X. Sun, *Catal. Today*, 147S, S46–S50 (2009).
7) S. M. Morris, P. F. Fulvio and M. Jaroniec, *J. Am. Chem. Soc.*, 130, 15210–15216 (2008).
8) R.-H. Zhao, C. P. Li, F. Guo and J.-F. Chen, *Ind. Eng. Chem. Res.*, 46, 3317–3320 (2007).
9) M. Kuemmel, D. Grosso, C. Boissiere, B. Smarsly, T. Brezesinski, P. A. Albouy, H. Amenitsch and C. Sanchez, *Angew. Chem., Int. Ed.*, 44, 4589–4592 (2005).
10) J. H. Kim, K. Y. Jung, K. Y. Park and S. B. Cho, *Microporous Mesoporous Mater.*, 128, 85–90 (2010).
11) J. Čejka, *Appl. Catal., A*, 254, 327–338 (2003).
12) Y. Lu, H. Fan, A. Stump, T. L. Ward, T. Rieker and C. J. Brinker, *Nature*, 398, 223–226 (1999).
13) H. Fan, F. V. Swol, Y. Lu and C. J. Brinker, *J. Non-Cryst. Solids*, 285, 71–78 (2001).
14) M. T. Bore, S. B. Rathod, T. L. Ward and A. K. Datye, *Langmuir*, 19, 256–264 (2003).
15) J. E. Hampsey, S. Arsenault, Q. Hu and Y. Lu, *Chem. Mater.*, 17, 2475–2480 (2005).
16) Y. Yamauchi, P. Gupta, K. Sato, N. Fukata, S. Todoroki, S. Inoue and S. Koshimoto, *J. Ceram. Soc. Japan*, 117, 198–202 (2009).
17) C.-K. Tsung, J. Fan, N. Zheng, Q. Shi, J. Forman, J. Wang and G. D. Stucky, *Angew. Chem., Int. Ed.*, 47, 8682–8686 (2008).
18) C. Boissière, L. Nicole, C. Gervais, F. Babonneau, M. Antonietti, H. Amenitsch, C. Sanchez and D. Grosso, *Chem. Mater.*, 18, 5238–5243 (2006).
19) IUPAC Commission on Colloid and Surface Chemistry Including Catalysis, *Pure Appl. Chem.*, 57, 603–619 (1985).
20) Q. Liu, A. Wang, X. Wang and T. Zhang, *Microporous Mesoporous Mater.*, 100, 35–44 (2007).
21) Q. Liu, A. Wang, X. Wang and T. Zhang, *Microporous Mesoporous Mater.*, 92, 10–21 (2006).